The EMBO Journal Vol.17 No.5 pp.1362–1370, 1998

Gelsolin is a downstream effector of rac for fibroblast motility

Toshifumi Azuma, Walter Witke, Thomas P.Stossel, John H.Hartwig and David J.Kwiatkowski[1]

Division of Experimental Medicine, Division of Hematology-Oncology, Department of Medicine, Brigham and Women's Hospital, Harvard Medical School, 221 Longwood Avenue, Boston, MA 02115, USA

[1]Corresponding author
e-mail: kwiatkowski@calvin.bwh.harvard.edu

Rac, a member of the rho family of GTPases, when activated transmits signals leading to actin-based membrane ruffling in fibroblasts. Compared with wild-type fibroblasts, gelsolin null (Gsn$^-$) dermal fibroblasts have a markedly reduced ruffling response to serum or EGF stimulation, which signal through rac. Bradykinin-induced filopodial formation, attributable to activation of cdc42, is similar in both cell types. Wild-type fibroblasts exhibit typical lamellipodial extension during translational locomotion, whereas Gsn$^-$ cells move 50% slower using structures resembling filopodia. Multiple Gsn$^-$ tissues as well as Gsn$^-$ fibroblasts overexpress rac, but not cdc42 or rho, 5-fold. Re-expression of gelsolin in Gsn$^-$ fibroblasts by stable transfection or adenovirus reverts the ruffling response, translational motility and rac expression to normal. Rac migrates to the cell membrane following EGF stimulation in both cell types. Gelsolin is an essential effector of rac-mediated actin dynamics, acting downstream of rac recruitment to the membrane.

Keywords: actin/gelsolin/rac/motility/ruffling

Introduction

The recent convergence of two research programs promises to advance our understanding of the cell surface movements involved in cell motility and shape changes. One of these fields concerns cellular actin assembly, fundamental to nearly all cell surface movements, and its regulation by actin-binding proteins. The other encompasses the spectrum of GTPases involved in cell signal transduction. GTPases, especially the rac, rho and cdc42 members of the ras superfamily and their numerous binding partners, appear to contribute importantly to the way in which particular surface stimuli elicit specific types of actin restructuring phenomena that lead to specific cell protrusions (Ridley and Hall, 1992; Ridley *et al*., 1992; Nobes and Hall, 1995; Tapon and Hall, 1997). Since actin is the structural element that establishes and maintains the architecture of surface protrusions, the factors directly regulating actin assembly and the three-dimensional configurations of assembled actin most likely operate downstream of the GTPases. Although numerous proteins have been identified which interact with rho GTPases (for reviews see Lamarche and Hall, 1994; Cerione and Zheng, 1996; Macara *et al*., 1996; Tapon and Hall, 1997), the challenge is to better establish the connections between GTPases and actin assembly.

The GTPase which appears most likely to control cell surface protrusive activity associated with translational locomotion is rac (Ridley *et al*., 1992). Overexpression of constitutively active rac promotes the formation of ruffling lamellae, which classically appear at the leading edge of crawling fibroblasts. In contrast, constitutively active cdc42 elicits extension of hairlike filopodia (Kozma *et al*., 1995; Nobes and Hall, 1995), but these structures can progress to lamellae and appear early during translocational motility in many cell types. Constitutively active rho causes formation of adhesion plaques and bundles of actin filaments (stress fibers) (Ridley and Hall, 1992), but since the abundance and size of these structures correlate negatively with cell locomotion (Herman *et al*., 1981), rho seems more likely to be involved in adhesion than locomotive responses to external stimulation.

Actin-regulating proteins that cap the fast growing ends of filaments are potentially downstream of rac in the pathway to actin assembly and locomotion (Schafer and Cooper, 1995; Barkalow *et al*., 1996). One founding member of the family of actin capping proteins is the ubiquitously expressed protein gelsolin (Yin and Stossel, 1979; Kwiatkowski *et al*., 1988). Gelsolin, activated by calcium ions and/or protons, severs the noncovalent bonds between actin subunits in a filament, thereby promoting rapid actin filament shortening (Yin and Stossel, 1979; Yin *et al*., 1981). After severing, gelsolin binds avidly to the fast-growing (barbed) ends of actin filaments, preventing filament elongation. Activated gelsolin can also nucleate actin filament assembly from monomers, creating filaments capped at the barbed end and growing at the pointed end. D3 and D4 phosphoinositides (PPI) remove gelsolin from actin filament barbed ends, permitting filament elongation (Janmey and Stossel, 1987; Hartwig *et al*., 1995). These *in vitro* observations provide a rationale for the importance of gelsolin in actin dynamics *in vivo*.

To explore gelsolin's *in vivo* role, we recently generated mice null for gelsolin by gene knockout techniques (Witke *et al*., 1995). Analysis of the mice demonstrated the importance of gelsolin in the dynamic actin responses of blood platelets and leukocytes, although the mice had normal development and viability. In addition, although tissue architecture appeared normal in the mice, their cultured fibroblasts had large actin stress fiber bundles and reduced motility in Boyden chamber and tissue culture wounding models.

In this paper we describe results that point to a close relationship between rac and gelsolin in the control of actin assembly and locomotion. All cells and tissues that

Table I. FITC-Dextran and horseradish peroxidase uptake by Gsn⁻, WT and revertant (G1) dermal fibroblasts. Absorbance per ml of extract is shown

Cell	FITC-dextran			Horseradish peroxidase		
	control	+EGF	+PDGF	control	+EGF	+insulin
WT	7.0 ± 2.0	11.0 ± 2.4	10.9 ± 1.0	0.29 ± 0.15	1.31 ± 0.60	1.01 ± 0.57
Gsn⁻	2.2 ± 0.5	2.8 ± 1.1	3.0 ± 1.0	0.22 ± 0.12	0.52 ± 0.20	0.27 ± 0.15
G1	7.6 ± 1.9	12.7 ± 2.0	11.5 ± 2.2			

normally express gelsolin have a compensatory overexpression of rac in Gsn⁻ animals. Despite rac overexpression, Gsn⁻ fibroblasts have markedly depressed ruffling activity and motility, although EGF stimulation translocates rac from the perikaryon to the cell periphery in normal fashion. Re-expression of gelsolin in these cells normalizes motility and rac expression, confirming that the lack of gelsolin leads directly to the overexpression of rac. These findings establish that gelsolin is a downstream effector of rac for motility, and that absence of gelsolin influences rac expression.

Results

Motility in Gsn⁻ dermal fibroblasts

We have previously demonstrated that tissue culture wound healing and Boyden chamber transmigration were significantly impaired in Gsn⁻ adult dermal fibroblasts in comparison with wild-type (WT) controls of similar origin (Witke *et al*., 1995). Since membrane ruffling is a process closely linked to cell crawling activity and can be measured quantitatively using assays of macropinocytosis, we investigated macropinocytosis in these cells using the tracking compounds FITC-dextran and HRP-peroxidase (Table I). Unstimulated uptake of FITC-dextran from the media was markedly reduced in Gsn⁻ fbroblasts compared with WT cells and the difference between the two cell types was accentuated by application of EGF or PDGF. Similar differences in stimulated uptake were seen when HRP-peroxidase was used as the tracking compound (Table I). Similar qualitative observations were made for uptake of Lucifer Yellow.

To investigate the motility of these cells in greater detail, videomicroscopy was used. Figure 1 provides a representative panel of frames of Gsn⁻ and WT cells, which were initially serum-starved and then stimulated with EGF and followed for 15 min. Several regions of ruffling activity can be seen in the WT cell over the 15 min interval (large arrows). In contrast, the Gsn⁻ cell is larger and flatter and displays no ruffling activity in any region. Motility differences could also be appreciated in co-culture experiments (Figure 2). When Gsn⁻ and WT fibroblasts were cultured on the same coverslip, serum-starved and then stimulated with EGF, ruffles containing gelsolin in the WT cells could be appreciated, whereas the Gsn⁻ cells had no ruffles.

Since the Gsn⁻ cells had previously been shown to move at about half the rate of WT cells in a tissue culture wounding model, we monitored these cells by videomicroscopy after wounding to assess their translocational motility. Linear wounds were made in a subconfluent dish of cultured cells and the cells were monitored in the constant presence of serum over 12 h (Figure 3). WT cells translocated through a process involving regions of peripheral ruffling, followed by a broad lamellar protrusion and attachment to the substratum, followed by migration of the nucleus and retraction of the tail of the cell. The Gsn⁻ cells moved much less in general than the WT cells and those which did move proceeded through a different progression. Cell protrusions occurred without ruffling activity and were much narrower in shape, though larger than classic filopodia or microspikes. Following extension of these narrow protrusions there was a broadening of the protrusion with attachment to substratum and forward movement of the cell body with delayed retraction of the tail. Measurement of nuclear translocation in these video images confirmed a reduced rate of movement in the Gsn⁻ cells compared with WT. WT cells moved at 0.902 ± 0.164 μm/s; Gsn⁻ cells moved at 0.514 ± 0.171 μm/s ($P<0.01$, 10 cells each tracked).

Rac expression in Gsn⁻ dermal fibroblasts and animals: recovery with gelsolin transfection

Since the rac GTPase is implicated as a critical signalling intermediate in cells undergoing ruffling, we investigated expression of rac in Gsn⁻ cells. Monoclonal antibodies against rac were prepared through the use of the recombinant his-tagged protein as immunogen in mice. Several hybridomas secreting antibodies reactive with the immunogen were identified, and monoclonal 7G3 was used for all further studies presented here. Specificity of this monoclonal antibody was demonstrated by immunoblot and ELISA binding to bacterially expressed rac, and lack of binding to similarly expressed rhoA or cdc42a, as well as its identification of a single 21 kDa band in immunoblot analysis of human and murine tissues.

Immunoblot analysis demonstrated that rac was overexpressed by ~5-fold in cultured Gsn⁻ dermal fibroblasts and aortic smooth muscle cells, in comparison with WT cells (Figure 4A, left). To confirm that this observation did not occur as an artifact related to culturing of the cells, analyses of murine tissue extracts were performed (Figure 4A, right). Ten Gsn⁻ and WT tissues demonstrated a consistent difference in the expression of rac, again with an ~5-fold increase in the Gsn⁻ tissues. Rac expression was variable from tissue to tissue in WT animals, as expected. A mild increase in rac expression in Gsn⁻ liver was also seen, even though gelsolin expression was below the detection limit in this particular immunoblot. We examined the livers of these animals by immunohistochemistry, using antibodies against gelsolin and rac. We observed expression of both proteins predominantly in the bile duct and arterial vascular cells, with increased rac expression in these cells in the Gsn⁻ liver (data not shown).

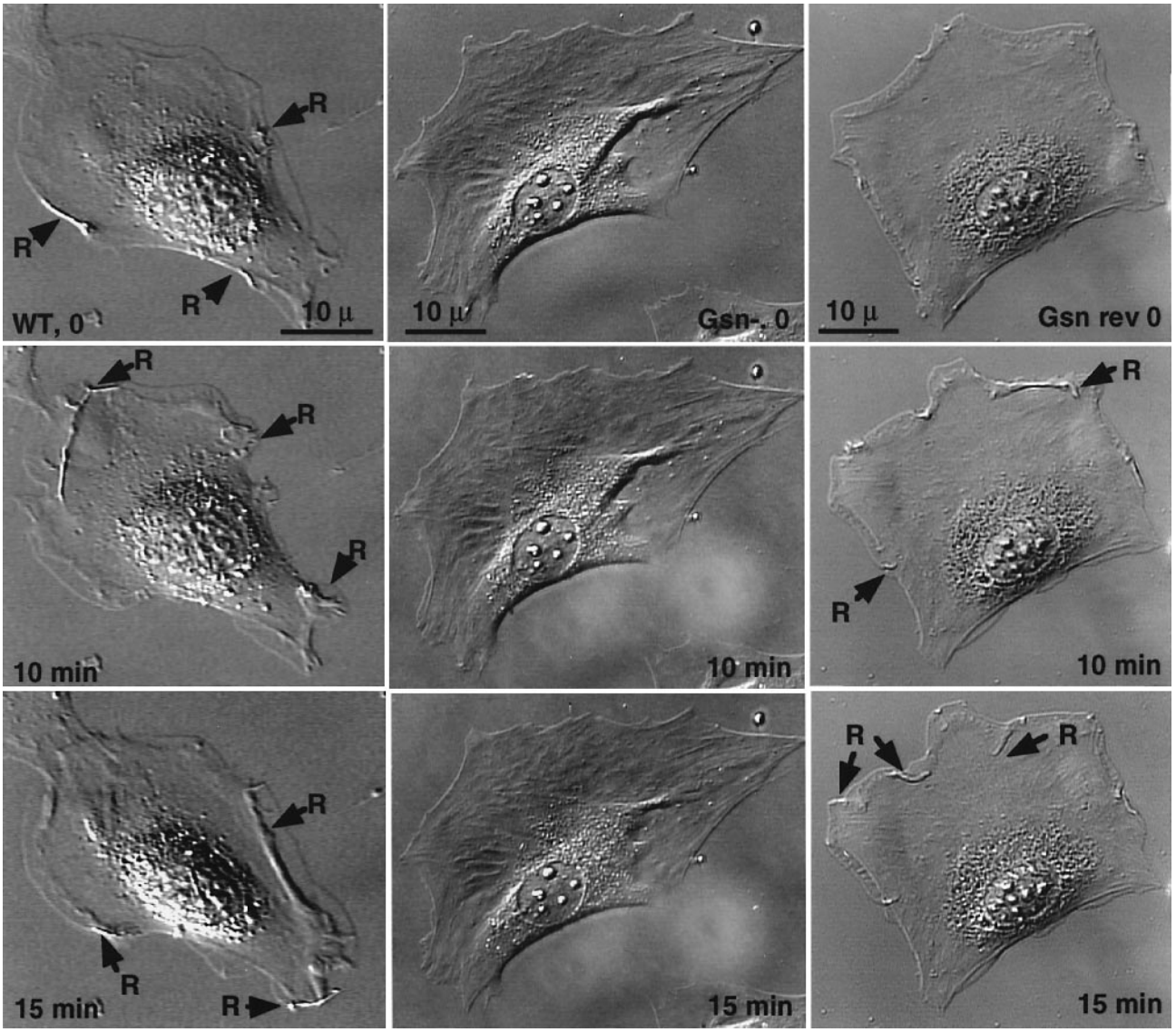

Fig. 1. Motility of Gsn$^-$ and WT dermal fibroblasts. Frames collected at 0, 10 and 15 min intervals after application of EGF (100 ng/ml) to serum-starved cells are shown, demonstrating ruffling activity (R, arrows) in the WT cells (left), and the gelsolin-expressing Gsn$^-$ cells transfected by adenovirus (right), but not in the Gsn$^-$ cells (middle).

To establish a direct connection between gelsolin expression and increased rac expression in the dermal fibroblasts, a gelsolin expression vector was transfected into the Gsn$^-$ cells and stable transfectant lines obtained. As shown in Figure 2D, gelsolin expression was restored to levels similar to those seen in WT fibroblasts. Notably, rac expression reverted to normal levels in the gelsolin-transfected cell lines. Analysis of these revertant Gsn$^+$ lines showed that they were now smaller in volume and spread size, comparable with WT fibroblast cells, and that they displayed increased motility (Figure 4D) in a tissue culture wounding assay. The wound closure rate of the revertant gelsolin-expressing cells surpassed that of the WT cells in some cases, and roughly correlated with the level of gelsolin expression, similar to what we have previously seen in NIH-3T3 cells (Cunningham *et al*., 1991). The lack of a perfect correlation between gelsolin expression levels and motility in these sublines is due, we suspect, to spontaneous drift in the motility phenotype of these clonal cell populations, reflecting their extended passage.

To confirm a causal connection between lack of gelsolin and increased rac and motility, we also re-introduced gelsolin expression into Gsn$^-$ fibroblasts through the use of a recombinant gelsolin-expressing adenovirus. As shown in Figure 1 (right), gelsolin-expressing, adenovirus-infected Gsn$^-$ cells displayed ruffling activity in response to EGF after serum starvation that was similar to that seen in WT fibroblasts. In contrast, control adenovirus-infected cells showed no increase in ruffling activity under similar stimulation (data not shown). Concomitant with the recovery of gelsolin expression, rac expression also declined to normal in the gelsolin-expressing, adenovirus-infected cells (Figure 4C).

Bradykinin signalling in Gsn$^-$ cells: cdc42 and rhoA expression

To examine signalling through cdc42, we stimulated serum-starved cells with bradykinin, and examined filopodial formation by videomicroscopy (Figure 5). In both Gsn$^-$ and WT cells filopodia appeared, but at lower levels

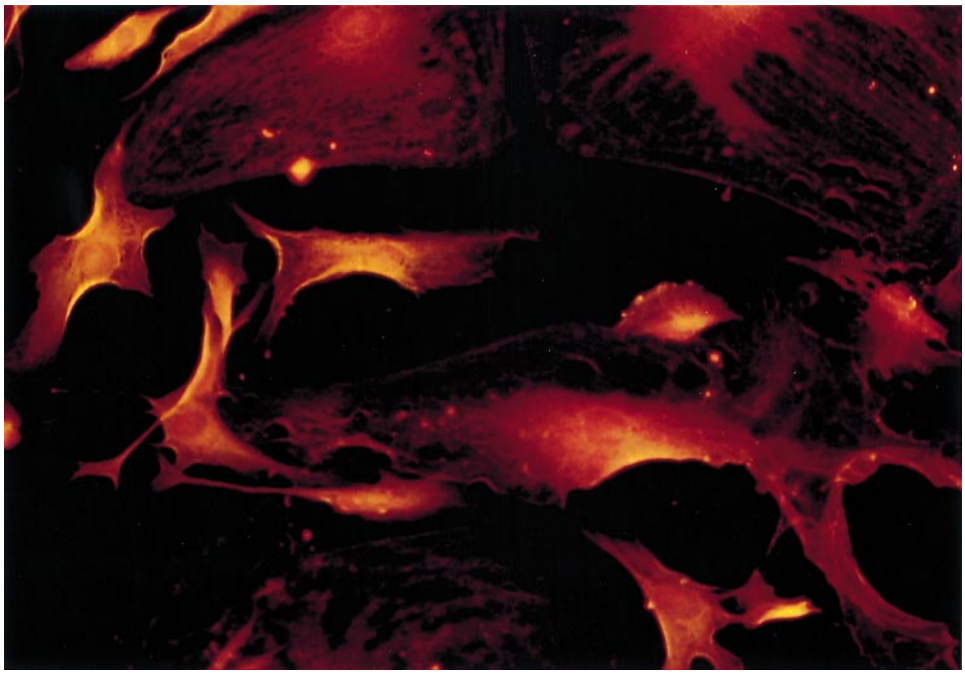

Fig. 2. EGF stimulation of co-cultured WT and Gsn$^-$ fibroblasts. Fluorescence images are shown with TRITC-phalloidin (red) used to identify actin filaments and FITC-conjugated secondary antibody (green) to identify gelsolin. Three large Gsn$^-$ cells are seen at top (2 cells) and bottom (1 cell), and several WT cells are seen in the middle. Gsn$^-$ cells are red and without ruffles, while WT cells are red/yellow with bright yellow ruffles indicative of focal concentration of actin and gelsolin.

than reported in Swiss 3T3 cells (Kozma *et al*., 1995; Nobes and Hall, 1995) probably reflecting differences in strain and tissue of origin. The numbers of filopodia did not differ significantly between the WT and Gsn$^-$ cells (0.29 ± 0.13 per cell versus 0.21 ± 0.07 per cell respectively). In the Gsn$^-$ cells filopodia did not progress to ruffling activity, consistent with the lack of response to EGF and PDGF seen above. In the WT cells progression of filopodial to ruffling activity could be seen in most cells, although the ruffling activity was not as striking as was seen following stimulation with PDGF or EGF. Expression levels of cdc42 and rhoA in Gsn$^-$ and WT fibroblasts were indistinguishable (Figure 4B).

Signalling through rac in the Gsn$^-$ dermal fibroblasts

To explore the mechanism of arrest of cell motility in dermal fibroblasts we examined the *in situ* distribution of rac and the kinetics of actin nucleation in WT and Gsn$^-$ cells. Antibody staining with the anti-rac antibody demonstrated that in resting, serum-deprived cells, rac was seen in both WT and Gsn$^-$ cells in a perinuclear location (Figure 6, top level). In response to EGF stimulation (Figure 6, second and third levels), in both cells there was migration of rac to the cell periphery, with focal concentration in WT cells in regions that were undergoing ruffle formation. Rac was also clearly overexpressed in the Gsn$^-$ cells in comparison with WT cells. Therefore, recruitment of rac to the cell membrane occurs in both cell types appropriately but downstream events are impeded in the Gsn$^-$ cells. Treatment of both cell types with wortmannin (Arcaro and Wymann, 1993) prior to EGF stimulation blocked the movement of rac to the cell membrane in both cell types (Figure 6, bottom level). This observation suggests that PI 3-kinase is involved in rac translocation, and that again both the Gsn$^-$ and WT cells could perform this event, implicating gelsolin's effect as downstream to these early events in rac-mediated signalling for motility.

To examine actin dynamics in these two cell populations in response to EGF stimulation, quiescent cells in suspension were treated with EGF and actin nucleation sites were measured in a pyrene-actin fluorimetric assay (Hartwig *et al*., 1995). As shown in Figure 7, the actin monomer assembly rate in unstimulated Gsn$^-$ cells was reduced compared with WT cells and showed no change following EGF stimulation. The actin monomer assembly rate in unstimulated WT cells was higher, and rose 3-fold 5 min after treatment with EGF. Assembly in the WT cells was completely inhibited by the addition of cytochalasin B to the assay, demonstrating that actin monomers were being assembled at the barbed end of actin nuclei only. Both Gsn$^-$ and WT cells responded to treatment with bradykinin during a 10 min interval with a ~3-fold increase in actin monomer assembly rate.

Discussion

We have provided evidence that gelsolin is a necessary downstream protein molecule ('effector') required for motility signalling through rac in adult murine dermal fibroblasts. First, there is a decrease in motile activity in the Gsn$^-$ cells compared with WT as measured by several motility assays. Secondly, this defect is repaired by expression of gelsolin at normal levels in the Gsn$^-$ cells. Thirdly, rac expression is increased in the Gsn$^-$ cells, and despite this overexpression, motility is still reduced; overexpression is reverted by expression of gelsolin in the same cells. Fourthly, rac overexpression is also seen in multiple tissues derived from the adult Gsn$^-$ mouse. Finally, Gsn$^-$ cells fail to respond to EGF by exposure of actin barbed

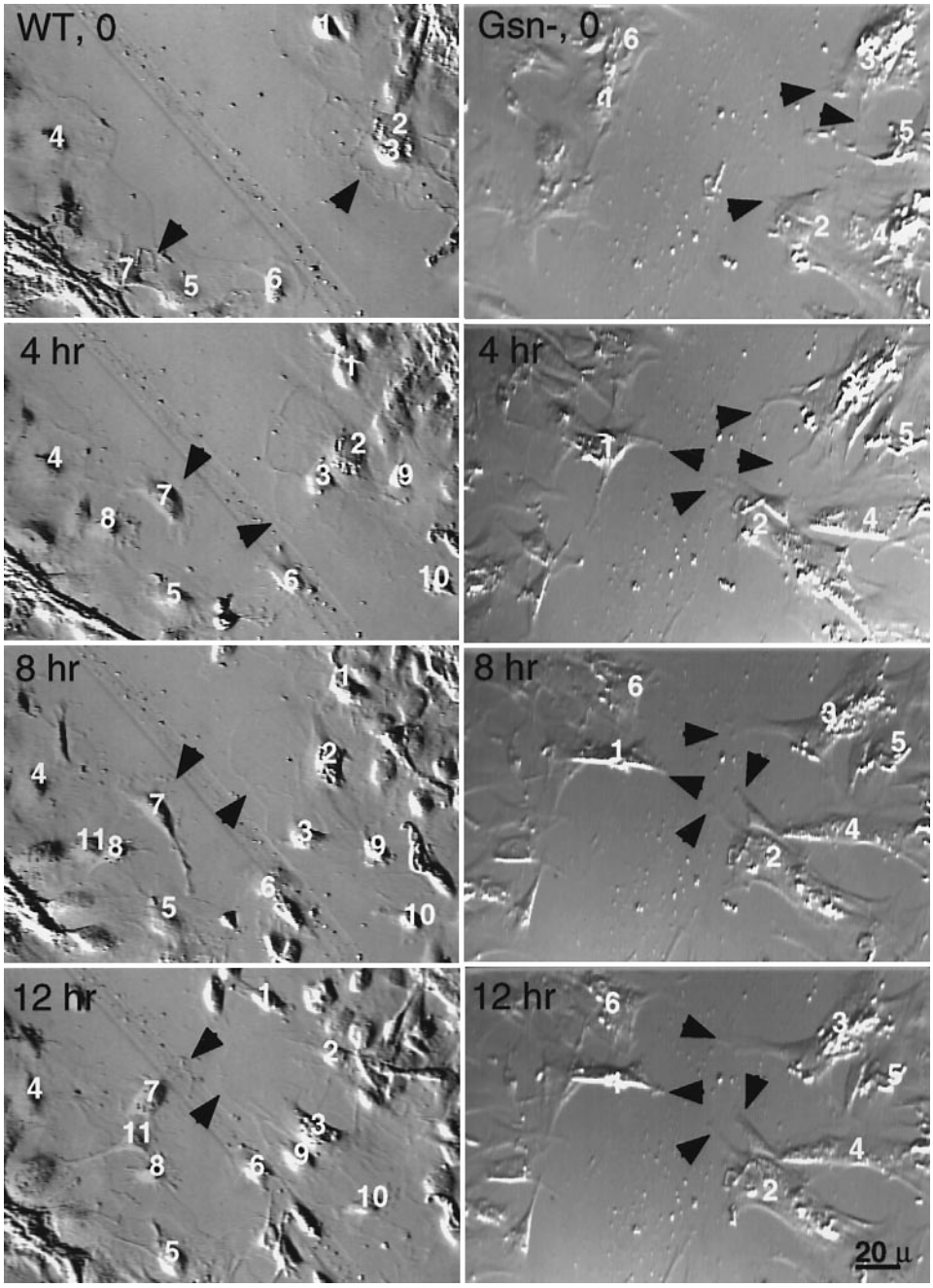

Fig. 3. Videomicroscopy analysis of Gsn⁻ and WT fibroblast response to tissue culture wounding. Frames collected at 4 h intervals after creation of a wound in a subconfluent population are shown. WT fibroblasts (left) demonstrate both more translocation and a broad leading edge (arrowheads). Gsn⁻ fibroblasts (right) demonstrate less translocation and narrow regions of protrusion (arrowheads) that gradually broaden.

end nuclei. These actin polymerization sites therefore drive actin assembly in ruffles. The results indicate that lack of gelsolin results in a pronounced defect in rac-mediated motility in these cells. Rac overexpression occurs, apparently in compensation for the reduction in motility, but is incompletely effective in relieving the motility defect. High level rac expression may account for the ability of the Gsn⁻ cells to translocate by extension of blunt filopodia (Figure 3). 'Run-off' stimulation of rho, also downstream of rac, could partially explain the abundant actin stress fibers present in the Gsn⁻ cells, although in quiescent Gsn⁻ cells we saw no evidence of constitutive rac activation as indicated by rac translocation to the membrane.

Actin polymerization is a necessary component of most forms of cell movement involving the leading edge of the cell, including protrusive activity and ruffling (Condeelis, 1994). The process of cell crawling or translocation involves other cellular activities in addition to actin polymerization, including adhesion events, force generation, release of adhesion complexes and retraction in the posterior portion of the cell (Lauffenburger and Horwitz, 1996; Mitchison and Cramer, 1996). Actin polymerization *in vivo* appears to be a complex process, involving associated proteins with at least three potential activities: (i) creation of an actin nucleation complex or release of a barbed end of a pre-existing filament, both to serve as sites for rapid addition of actin monomers; (ii) provision

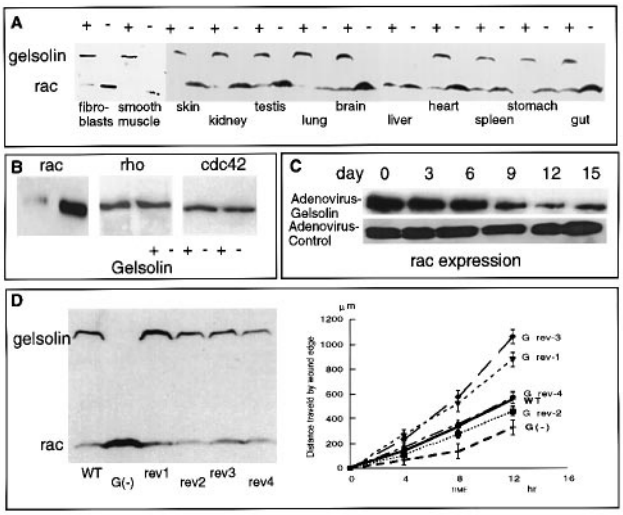

Fig. 4. Rac expression in Gsn⁻ fibroblasts and recovery by transfection of gelsolin. (**A**) Rac expression assessed by immunoblot in cultured dermal fibroblasts, aortic smooth muscle cells and tissues from Gsn⁻ and WT mice. (**B**) Comparison of rac, rho, and cdc42 expression in Gsn⁻ and WT dermal fibroblasts by immunoblot. (**C**) Adenovirus-mediated gelsolin expression in Gsn⁻ dermal fibroblasts results in reversion of rac overexpression. (**D**) Gelsolin expression by stable transfection in Gsn⁻ dermal fibroblasts results in reversion of rac overexpression (left) and recovery of motility (right).

of actin monomers charged with ATP for incorporation in filaments; and (iii) F-actin binding ability to organize actin polymers into three dimensional arrays as required for the particular type of cell process being generated.

The source of actin filament nucleation sites or barbed ends for actin assembly into filaments has been widely debated (Lauffenburger and Horwitz, 1996; Welch *et al*., 1997) and is difficult to examine *in vivo*. In platelets there is good evidence for a critical role for gelsolin. Gelsolin severs actin filaments during an initial Ca^{2+} flux in platelets and then is released by a rac-mediated rise in PPIs of the D4 type. This creates the actin nucleating sites that appear during the shape change reaction (Hartwig *et al*., 1995). The increase in D4-containing PPIs also blocks the binding of other PPI sensitive barbed end binding proteins (capping protein, capG) during this process (Schafer and Cooper, 1995; Barkalow *et al*., 1996). Our observations suggest that gelsolin also mediates the formation of sites for rapid actin polymerization during cell protrusive and ruffling activity in murine dermal fibroblasts. The formation of actin microspikes and actin assembly observed in Gsn⁻ cells following stimulation with bradykinin indicates that cdc42-mediated signalling follows a different pathway, not involving gelsolin. It also demonstrates that other critical components for actin assembly are present and functional in the Gsn⁻ cells, including actin monomers and the family of proteins that modulate assembly of actin monomers into filaments such as profilins, thymosins, cofilin and others (Sun *et al*., 1995; Carlier *et al*., 1997). These results are also consistent with recent observations in which gelsolin did not appear necessary for *Listeria* motility in *Xenopus* oocytes (Rosenblatt *et al*., 1997).

Previous studies in neutrophils have demonstrated the translocation of rac from the cytosol to membrane fractions following stimulation (Bokoch *et al*., 1994), but direct *in situ* evidence for rac movement has not been obtained. In quiescent fibroblasts, we observed rac in a central, perinuclear location, correlating with the inactive state, and its translocation to the cell periphery to apparent regions of ruffling activity upon stimulation. Wortmannin completely blocked this translocation, indicating that it is dependent on PIP3 generation (Arcaro and Wymann, 1993). The translocation could be a diffusion driven process, following release of racGTP from rhoGDI, were a favorable site for racGTP binding created at sites to become ruffles, but could also be mediated by an adapter protein, such as grb2 for ras (Bourne *et al*., 1991). The specific association of rac to regions of ruffles, suggests that a specific transport and/or binding mechanism is involved.

Based upon these observations we propose the following model for induction of ruffling and motility in normal WT fibroblasts. EGF interaction with receptor leads to activation of PI 3-kinase (Hawkins *et al*., 1995; Rameh *et al*., 1995) which, by some as yet undefined mechanism, leads to activation and recruitment of rac to membrane sites where ruffling and motility are to occur. Activated rac at the membrane recruits a multi-protein complex including PI(4)P-5 kinase (Tolias *et al*., 1995), and stimulates $PI(4,5)P_2$ synthesis. Calcium ion or proton transients and regulated changes in $PI(4,5)P_2$ levels lead to cycles of activation of gelsolin, correlating with severing and partial dissolution of existing actin filament networks, and inactivation providing actin filament nucleation sites for actin assembly. Our demonstration that both rac and gelsolin are recruited to the sites of ruffling activity (Figures 2 and 6) suggests the possibility of physical interaction between gelsolin and rac with membrane lipids in these regions.

The upregulation of rac in the Gsn⁻ animals and cells indicates that some mechanism exists for regulation of expression of this gene and protein. Presumably regulation of rac expression occurs due to some feedback mechanism that senses the motile capacity or actin organization of the cell. Such regulation is unusual among the major members of the ras and rho families of GTPases and exploration of its mechanism will be of considerable interest. In addition, the putative role of rac in transformation (Qiu *et al*., 1995) suggests the possibility that the Gsn⁻ animals will be at increased risk of developing malignancies. Thus far, without carcinogenic insult, no increase in tumor formation has been observed in these animals.

Materials and methods

Reagents

EGF (used at 100 ng/ml) and PDGF (used at 10 ng/ml) were purchased from R&D systems (Minneapolis, MN). Cytochalasin B, bradykinin (used at 100 ng/ml), FITC-labeled dextran, glutathione agarose beads, wortmannin (used at 10 nM), phallacidin, phenylmethylsulfonylfluoride (PMSF), horse radish peroxidase, Lucifer Yellow, and TRITC-labeled phalloidin were from Sigma (St. Louis, MO). His Bond Resin was obtained from Novagen (Madison, WI). Anti-cdc42 antibody was obtained from Santa Cruz Biotechnology.

Gsn⁻ mice and cell culture

The Gsn⁻ trait is maintained in mixed Sv129-BALB/c and Sv129-C57/bl backgrounds. Matched littermates that are $Gsn^{-/-}$ and WT, derived from $Gsn^{+/-}$ matings, are used for all experiments including cell line derivation.

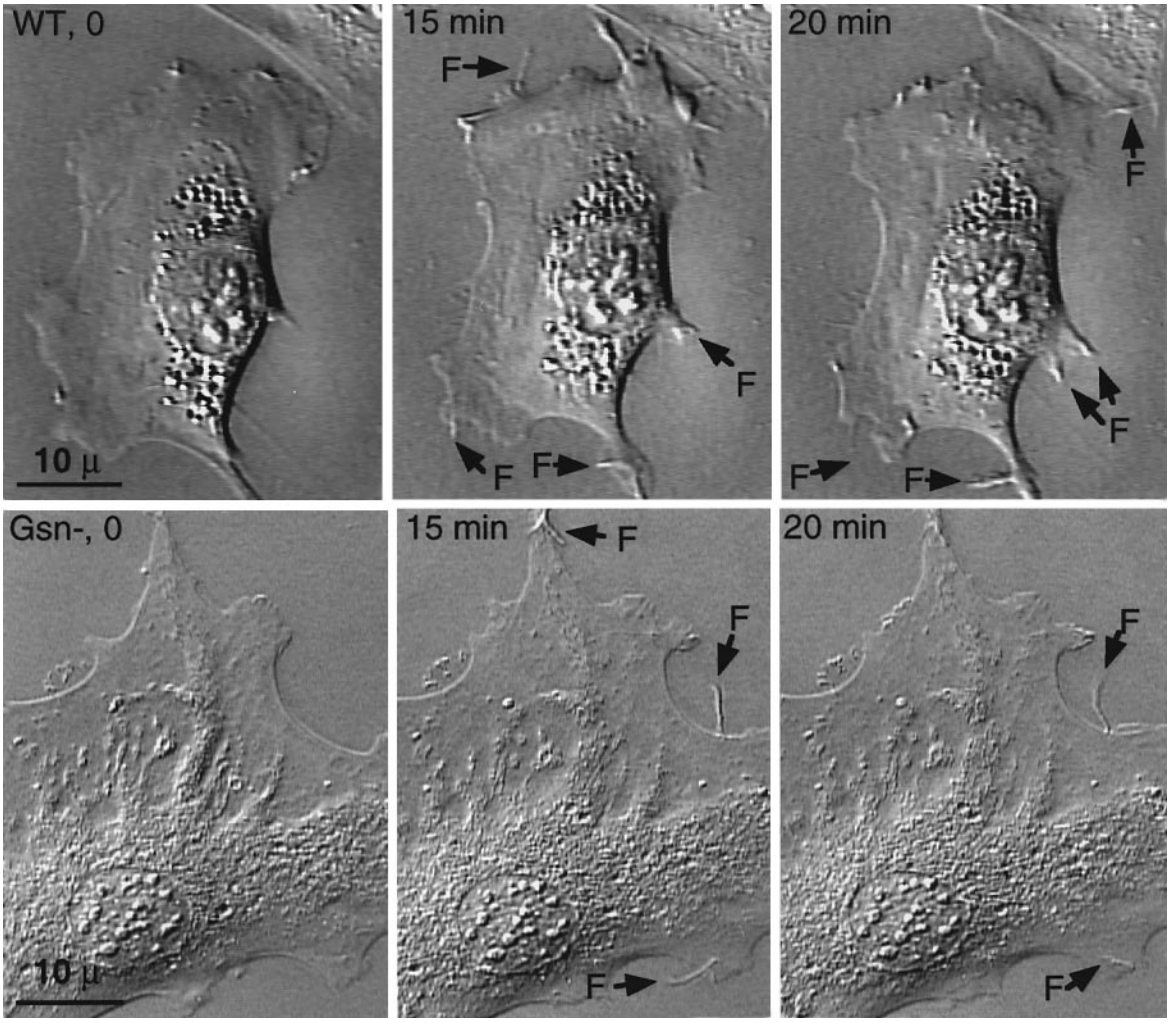

Fig. 5. Cdc42-mediated motility in Gsn⁻ fibroblasts. Frames collected at 0, 15 and 20 min after application of bradykinin (100 ng/ml) to serum-starved WT (top) and Gsn⁻ (bottom) cells demonstrate filopodia formation (arrows, F) in both cell types.

Tissue extracts from the mice were prepared by homogenization in 1% Triton X-100, 50 mM Tris–HCl, pH 7.5, 1 mM PMSF, 0.2 μg/ml aprotinin, 4 mM EDTA. Dermal fibroblasts are cultured as explants from the abdominal and dorsal cutaneous tissue of 1–2 month old mice and were maintained in Dulbecco's modified Eagle's medium (DMEM) (Gibco-BRL) supplemented with 10% fetal calf serum. Cultured cells were used for all experiments by culture passage 2, apart from the clonally gelsolin-transfected sublines. Tissue culture motility measurements were made by wounding a subconfluent culture dish with an 18 gauge needle as described previously (Cunningham *et al*., 1991).

Videomicroscopy

Cells were plated onto 25 mm acid washed glass coverslips and serum starved for 16–24 h in CO_2 independent medium without serum. Coverslips were placed on the microscope stage and maintained at 37°C using a TC102 temperature controller and incubation chamber (Medical System Corp., Greenvale, NY). Differential interference contrast (DIC) microscopy was performed on a Zeiss Axiovert 405M inverted microscope with a 40×0.9 numerical aperture plan-neofluor lens. For time-lapse recordings, images were collected using a Hamamatsu C2400 video camera (Photonic Microscopy Inc., Bridgewater, NJ) and recorded on a Panasonic TQ-3038F video recorder.

Fluorescence microscopy

Cells grown on coverslips were fixed with 4% paraformaldehyde/PBS for 5 min at room temperature. Coverslips were rinsed in PBS and cells were treated with sodium borohydride (0.5 mg/ml) in PBS for 10 min and blocked with 5% normal goat serum/PBS for 60 min at room temperature. The coverslips were incubated with primary antibodies for 1 h at room temperature. After being washed with PBS five times, the coverslips were incubated with FITC-labeled goat anti-rabbit or anti-mouse antibody for 1 h at room temperature with or without added 100 ng/ml TRITC-phalloidin. The coverslips were rinsed five times with PBS and mounted onto glass slides using Aqua polymount (Polyscience) and viewed on an Olympus BH3 microscope.

Production and purification of recombinant proteins

RhoA, rac and cdc42 (G25 isotype) were expressed as glutathione *S*-transferase and/or six histidine fusion proteins in bacteria. A rhoA cDNA clone was a gift from S.Narumiya, Kyoto University; and a rac cDNA clone was a gift from A.Hall, University College London. A human cdc42 (G25k isoform) cDNA was obtained by PCR amplification of human brain cDNA, and confirmed by sequencing.

Generation of antibodies

Polyclonal anti-mouse gelsolin antibodies were prepared by immunizing rabbits with recombinant mouse gelsolin, and were affinity purified prior to use. Monoclonal antibodies (anti-rac and anti-rho) were produced according to standard procedures. In brief, 6-week-old BALB/c mice were immunized with bacterially expressed protein three times with adjuvant at 3 week intervals. Spleen cells were fused with mouse myeloma cell (SP2) and hybridoma clones secreting anti-rac or anti-rho antibodies were selected by ELISA and confirmed by immunoblotting of samples of all three recombinant proteins as well as cellular extracts.

Transfection methods

To express gelsolin in dermal fibroblasts, two methods were used. First, we subcloned the murine gelsolin cDNA into the expression vector LKH, electroporated 10^8 cells and selected stable transfectant cell lines using hygromycin B. Six clonal lines were derived, of which four stably

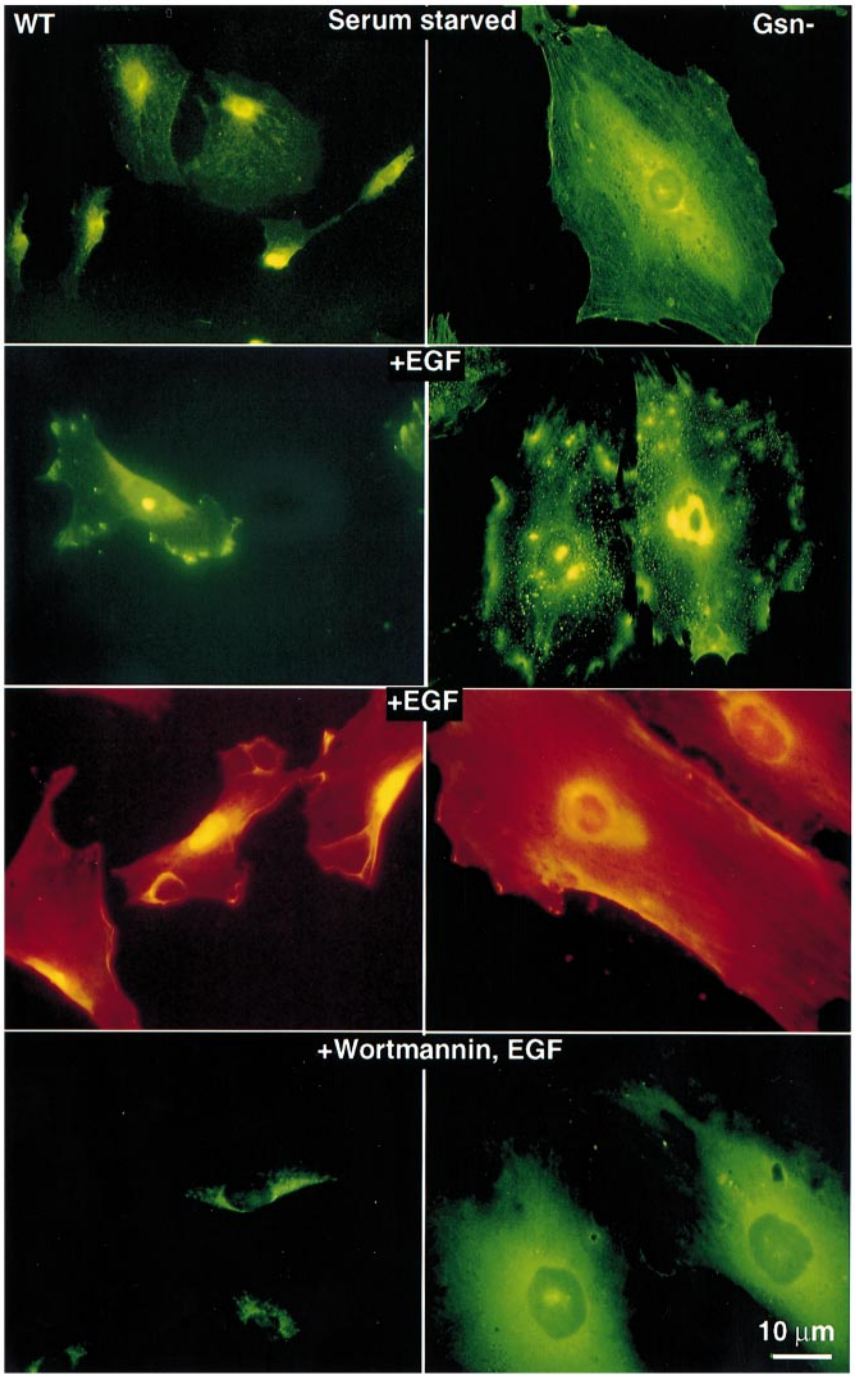

Fig. 6. Rac immunolocalization in WT and Gsn$^-$ cells. Fluorescence images are shown with FITC-conjugated secondary antibody (green) to identify rac and TRITC-phalloidin (red) used to identify actin filaments (third level only). Top level, serum starved cells; 2nd level, similar cells 10 min after addition of EGF at 100 ng/ml; 3rd level, identical to 2nd but with actin staining; bottom level, 30 min after addition of wortmannin at 10 nM and 10 min after addition of EGF at 100 ng/ml.

expressed murine gelsolin. Secondly, the murine gelsolin cDNA was cloned into the pacCMV vector which contains the CMV early promoter to drive transcription and a downstream fragment of the SV40 genome that includes the small t antigen intron and the polyadenylation signals. This gelsolin-containing plasmid and pJM17 were co-transfected into 293 cells. Recombinant adenovirus was isolated, titered and amplified as described (Becker *et al*., 1994).

Immunoblotting

Proteins were SDS–PAGE fractionated and transferred onto immobilon P membrane (Millipore Corporation, Bedford MA). Membranes were incubated in 50 mM Tris, 150 mM NaCl, 0.1% Tween 20 (TBS-T) (pH 8.0) containing 10% (w/v) non-fat dry milk at 4°C overnight followed by a 1 h incubation with an affinity-purified polyclonal (gelsolin, 1 μg/ml; cdc42 1 μg/ml) or monoclonal (rac, 50 ng/ml; rho, 100 ng/ml) antibody diluted in TBS-T, 5% dry milk (TTM). Following three rinses, horseradish peroxidase-conjugated goat anti-rabbit or anti-mouse antibody was diluted in TTM and added to the membranes for 60 min at room temperature. The membranes were then washed five times for 5 min and bound antibodies were detected using enhanced chemiluminescence (ECL).

Pinocytosis assays

Cells were plated at three different densities (2×10^4, 4×10^4 and 8×10^4 cells/25 mm dish). The cells were serum-starved overnight in DMEM and incubated in PBS at 37°C for 30 min. FITC-dextran, horse radish

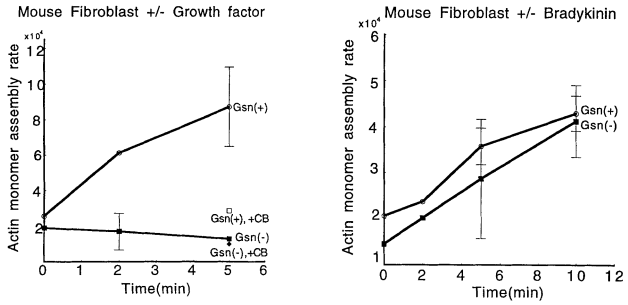

Fig. 7. Actin monomer assembly rates in Gsn$^-$ and WT dermal fibroblasts. The rate of assembly per cell, $\times 10^4$, is shown over 5–10 min after stimulation with EGF (left) or bradykinin (right).

peroxidase, or Lucifer yellow was added (final concentrations 2, 1 and 1 mg/ml, respectively) with or without EGF (10 ng/ml) and incubated at 37°C for 60 min. As a control the same set of cells were incubated at 4°C. After washing with chilled PBS three times, the cells were lysed in 50 mM Tris pH8.5, 0.1% Triton X-100 for 30 min at room temperature. Fluorescence measurements were made with a Perkin-Elmer LS50b fluorescence spectrophotometer to assess uptake of FITC-dextran (excitation 495 nm, emission 514 nm). Horse radish peroxidase activity was measured by incubation with *o*-diansidine at 0.1 mg/ml and quantitation of absorbance at 460 nm. Lucifer yellow uptake was assessed by fluorescence microscopy.

Measurement of actin filament ends

The number of exposed actin filament barbed ends was determined by measuring the rate and extent of pyrene-labeled actin polymerization in detergent lysates (Hartwig *et al*., 1995). Cells were cultured in conventional tissue culture dishes, serum-starved overnight, detached by treatment with 5 mM EDTA, and maintained as a suspension at 10^6 cells/ml at 37°C in DMEM. After stimulation with 10 ng/ml EGF or 100 ng/ml bradykinin, they were permeabilized with 0.1 volume of PHEM buffer (60 mM PIPES, 25 mM HEPES, 10 mM EGTA, and 2 mM $MgCl_2$ pH 7.4) containing 1% Triton X-100, 1 μM phallacidin, and protease inhibitors (Schliwa *et al*., 1981). To 100 μl of this detergent lysate, 185 μl of 100 mM KCl, 0.2 mM $MgCl_2$, 0.1 mM EGTA, 0.5 mM ATP, 10 mM Tris–HCl, 0.5 mM dithiothreitol pH 7.0 were added. Assembly of added pyrene-actin (final concentration 1 μM) into filaments was monitored with a Perkin-Elmer spectrophotometer at excitation and emission wave lengths of 366 and 386 nm, respectively. The data are expressed as actin assembly rate per cell (monomers into filaments/s) as previously described (Hartwig *et al*., 1995).

Acknowledgements

We thank Joel Swanson for assistance with the pinocytosis assays. This work was supported by grants from the NIH (HL48743 and HL54188).

References

Arcaro,A. and Wymann,M. (1993) Wortmannin is a potent phosphatidylinositol 3-kinase inhibitor; the role of phosphatidylinositol 3,4,5-triphosphate in neutrophil responses. *J. Biochem*., **296**, 297–301.

Barkalow,K., Witke,W., Kwiatkowski,D. and Hartwig,J. (1996) Coordinated regulation of platelet actin filament barbed ends by gelsolin and capping protein. *J. Cell Biol*., **134**, 389–399.

Becker,T.C., Noel,R.J., Coats,W.S., Gomez-Foix,A.M., Alam,T., Gerard,R.D. and Newgard,C.B. (1994) Use of recombinant adenovirus for metabolic engineering of mammalian cells. *Methods Cell Biol*., **43**, 161–189.

Bokoch,G., Bohl,B. and Chuang,T.-H. (1994) Guanine nucleotide exchange regulates membrane translocation of Rac/Rho GTP-binding proteins. *J. Biol. Chem*., **269**, 31674–31679.

Bourne,H., Sanders,D. and McCormick,F. (1991) The GTPase superfamily: conserved and molecular mechanism. *Nature*, **349**, 117–127.

Carlier,M.F. *et al*. (1997) Actin depolymerizing factor (ADF/cofilin) enhances the rate of filament turnover: implications in actin-based motility. *J. Cell Biol*., **136**, 1307–1323.

Cerione,R.A. and Zheng,Y. (1996) Dbl family of oncogenes. *Curr. Opin. Cell Biol*., **8**, 216–222.

Condeelis,J. (1994) Life at the leading edge: the formation of cell protrusions. *Annu. Rev. Cell Biol*., **9**, 411–444.

Cunningham,C., Stossel,T. and Kwiatkowski,D. (1991) Enhanced motility of NIH 3T3 fibroblasts that overexpress gelsolin. *Science*, **251**, 1233–1236.

Hartwig,J., Bokoch,G., Carpenter,C., Janmey,P., Taylor,L., Toker,A. and Stossel,T. (1995) Thrombin receptor ligation and activated Rac uncap actin filament barbed ends through phosphoinositide synthesis in permeabilized human platelets. *Cell*, **82**, 643–653.

Hawkins,P. *et al*. (1995) PDGF stimulates an increase in GTP-Rac via activation of phosphoinositide 3-ki9nase. *Curr. Biol*., **5**, 393–403.

Herman,I.M., Crisona,N.J. and Pollard,T.D. (1981) Relation between cell activity and the distribution of cytoplasmid actin and myosin. *J. Cell Biol*., **90**, 84–91.

Janmey,P. and Stossel,T. (1987) Modulation of gelsolin function by phosphatidylinositol 4,5-bisphosphate. *Nature*, **325**, 362–364.

Kozma,R., Ahmed,S., Best,A. and Lim,L. (1995) The Ras-related protein Cdc42Hs and bradykinin promote formation of peripheral actin microspikes and filopodia in swiss 3T3 fibroblasts. *Mol. Cell. Biol*., **15**, 1942–1952.

Kwiatkowski,D.J., Mehl,R., Izumo,S., Nadal-Ginard,B. and Yin,J.L. (1988) Muscle is the major source of plasma gelsolin. *J. Biol. Chem*., **263**, 8239–8243.

Lamarche,N. and Hall,A. (1994) GAPs for rho-related GTPases. *Trends Genet*., **10**, 436–440.

Lauffenburger,D. and Horwitz,A. (1996) Cell migration: a physically integrated molecular process. *Cell*, **84**, 359–369.

Macara,I., Lounsbury,K., Richards,S., McKiernan,C. and Bar-Sagi,D. (1996) The Ras superfamily of GTPases. *FASEB*, **10**, 625–630.

Mitchison,T.J. and Cramer,L.P. (1996) Actin-based cell motility and cell locomotion. *Cell*, **84**, 371–379.

Nobes,C. and Hall,A. (1995) Rac, rho and cdc42 GTPase regulate the assembly of multi-molecular focal complexes associated with actin stress fibers, lamellipodia, and filopodia. *Cell*, **81**, 53–62.

Qiu,R.G., Chen,J., Kirn,D., McCormick,F. and Symons,M. (1995) An essential role for rac in ras transformation. *Nature*, **374**, 457–459.

Rameh,L., Chen,S.-C. and Cantley,L. (1995) Phosphatidylinositol (3,4,5)P3 interacts with SH2 domains and modulates PI 3-kinase association with tyrosine-phosphorylated proteins. *Cell*, **83**, 821–830.

Ridley,A. and Hall,A. (1992) The small GTP-binding protein rho regulates the assembly of focal adhesions and actin stress fibers in response to growth factors. *Cell*, **70**, 389–400.

Ridley,A., Paterson,H., Johnston,C., Diekmann,D. and Hall,A. (1992) The small GTP-binding protein rac regulates growth factor-induced membrane ruffling. *Cell*, **70**, 401–410.

Rosenblatt,J., Agnew,B., Abe,H., Bamburg,J. and Mitchison,T. (1997) Xenopus actin depolymerizing factor/cofilin (XAC) is responsible for the turnover of actin filaments in Listeria monocytogenes tails. *J. Cell Biol*., **136**, 1323–1332.

Schafer,D.A. and Cooper,J.A. (1995) Control of actin assembly at filament ends. *Annu. Rev. Cell Dev. Biol*., **11**, 497–518.

Schliwa,M., van Blerkom,J. and Porter,K. (1981) Stabilization of the cytoplasmic ground substance in detergent-opened cells and a structural and biochemical analysis of its composition. *Proc. Natl Acad. Sci. USA*, **78**, 4329–4333.

Sun,H.-Q., Kwiatkowska,K. and Yin,H.L. (1995) Actin monomer binding proteins. *Curr. Opin. Cell Biol*., **7**, 102–110.

Tapon,N. and Hall,A. (1997) Rho, rac and cdc42 GTPases regulate the organization of the actin cytoskeleton. *Curr. Opin. Cell Biol*., **9**, 86–92.

Tolias,K., Cantley,L. and Carpenter,C. (1995) Rho family GTPases bind to phosphoinositide kinases. *J. Biol. Chem*., **270**, 17656–17659.

Welch,M., Mallavarapu,A., Rosenblatt,J. and Mitchison,T. (1997) Actin dynamics *in vivo*. *Curr. Opin. Cell Biol*., **9**, 54–61.

Witke,W., Sharpe,A., Hartwig,J., Azuma,T., Stossel,T. and Kwiatkowski,D. (1995) Hemostatic, inflammatory, and fibroblast responses are blunted in mice lacking gelsolin. *Cell*, **81**, 41–51.

Yin,H., Hartwig,J., Marayama,K. and Stossel,T. (1981) Ca^{2+} control of actin filament length. Effect of macrophage gelsolin on actin polymerization. *J. Biol. Chem*., **256**, 9693–9697.

Yin,H.L. and Stossel,T.P. (1979) Control of cytoplasmic actin gel-sol transformation by gelsolin, a calcium-dependent regulatory protein. *Nature*, **281**, 583–586.

Received August 1, 1997; revised December 17, 1997; accepted December 19, 1997